CHAPTER V
RESULTS AND DISCUSSION

5.1. Reaction Kinetics

5.1.1. Effect of the Concentration of Sodium Nitrite

To determine the reaction order with respect to $NaNO_2$, the concentration of NH_4Cl was held constant at 2.5 M while the concentration of $NaNO_2$ was varied at four different values of 0.15, 0.25, 0.4, and 0.5 M. The pH was also fixed at 3.5 by adding appropriate amounts of concentrated hydrochloric acid. The reaction for each concentration was then run for 3 minutes with the temperature being recorded every 10 seconds. Linear regression was applied on the temperature versus time trajectory to obtain the slope (initial reaction rate) for each concentration. Consequently, a log-log graph between the slope calculated versus the initial concentration revealed the coefficient (α - 1) following equation (3.11). Eventually, Figure 5.1 gives the reaction order with respect to sodium nitrite, α, to be approximately 3.1.

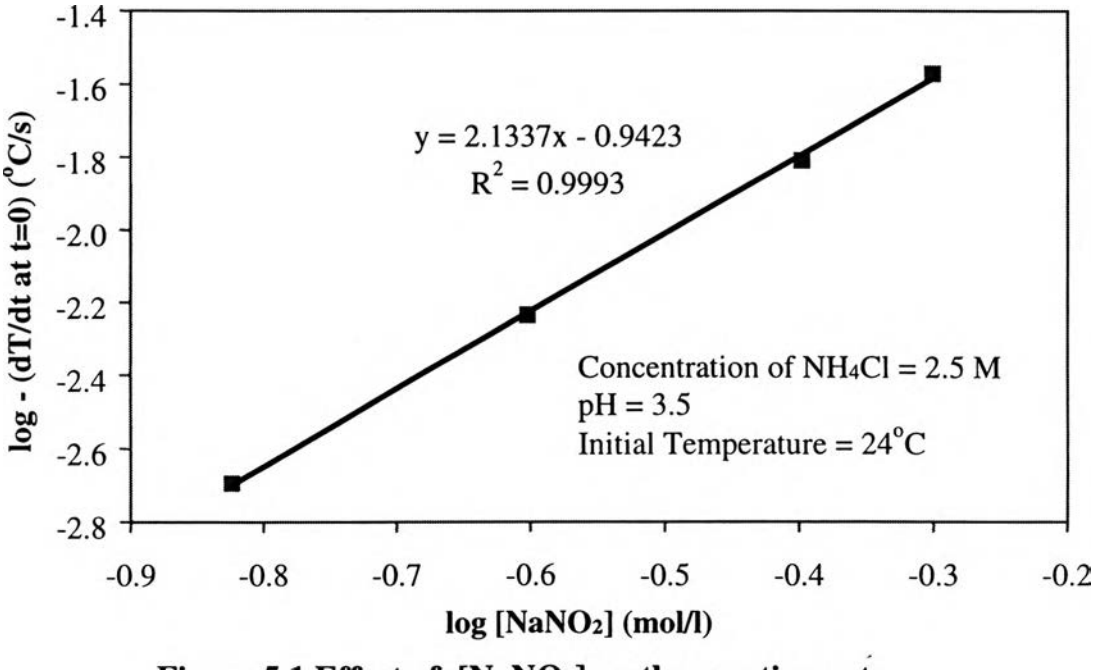

Figure 5.1 Effect of [$NaNO_2$] on the reaction rate.

5.1.2. Effect of the Concentration of Ammonium Chloride

Similarly, to determine the reaction order with respect to ammonium chloride, the concentration of ammonium chloride was simply varied at four different values of 0.15, 0.25, 0.4, and 0.5 M while the concentration of sodium nitrite was kept constant at 2.5 M. Also, the pH was held at 4.5 by adding appropriate amounts of concentrated hydrochloric acid. Figure 5.2 shows the natural log of the initial concentration versus the natural log of the initial slopes calculated from the temperature-time profiles. Eventually, using equation (3.12), the reaction order regarding to ammonium chloride in the rate law equation, β, is approximately 2.5.

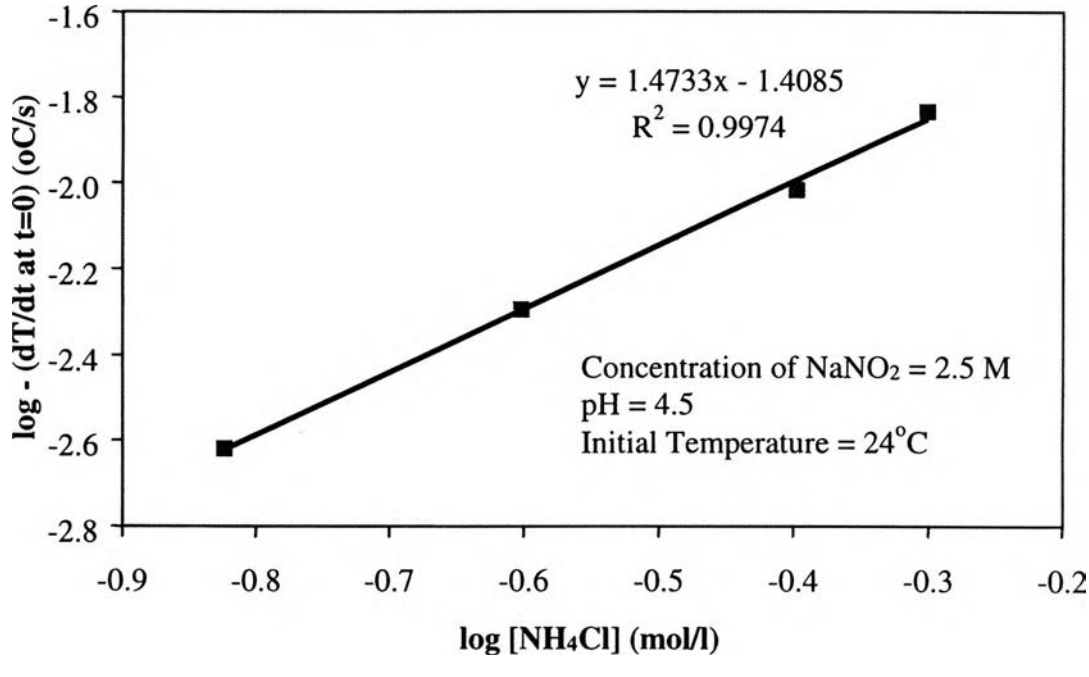

Figure 5.2 Effect of [NH_4Cl] on the rate of increasing temperature.

5.1.3. Effects of pH and Temperature of the Solution

To determine the rate constants and activation energies, the concentrations of both ammonium chloride and sodium nitrite were held constant at 2.5 M while the initial pH of the solution was varied using concentrated hydrochloric acid or sodium hydroxide pellets. pH values of 3.91, 4.66, and 4.90 were achieved by adding 1 ml, 0.25 ml, and 0.15 ml of

concentrated HCl, respectively whereas pH values of 7.40 and 7.65 were obtained by adding 0.08 g NaOH and 0.2 g NaOH, respectively. In addition, one run was conducted at a pH of 6.19, where neither HCl nor NaOH was added. There were difficulties in running the experiments at high and low pHs since the rate of the reaction is very slow at high pHs and very rapid at low pHs. The initial temperature, therefore, was raised to quite high values (up to 90°C) and lowered to rather low values (as low as –2°C) in order to get a measurable and more accurate data. As in the previous part, the temperature was recorded every ten seconds, this data was plotted as temperature-time trajectories, and then the slope of each line was calculated. Consequently, using equation (3.11), the value of $k_{t=0}$ was calculated for each run using the initial slope as $(dT/dt)_{t=0}$. The rate constants and activation energies, which are k_{00}, k_{01}, $k_{01,}$ $E_{0,}$, $E_{1,,}$ and E_2, were then obtained by using nonlinear regression in Mathcad for values of $k_{t=0}$ as different initial pHs and initial temperatures following the model specified in equation (3.13). Their values are listed in Table 5.1.

Table 5.1 Activation energies and rate constants of the reaction.

Rate Constant	Rate Constant $(dm^3/mol)^{5.5}s^{-1}$	Activation Energy (kcal/mol)	$[H^+]$ Order
k_0	8 E +9	23.8	-
k_1	5 E +13	13.9	1.8
k_2	-8 E +5	25.8	0.7

5.1.4. Summary of Reaction Kinetics

As shown in equations (3.7), (3.13) to (3.16), the rate law for the reaction between ammonium chloride and sodium nitrite is dependent on four variables of the concentrations of ammonium chloride and sodium nitrite, the

pH of the solution, and the temperature of the solution. By using the initial rate method, the reaction order with respect to sodium nitrite was found to be 3.1 while that of ammonium chloride was 2.4. The values of activation energies, rate constants, and orders with respect to concentration of proton in the solution are listed in Table 5.1.

In conclusion, the rate law can be written as follows:

$$-r_A = kC_A^{3.1} C_B^{2.5} \tag{5.1}$$

where

$$k = k_0 + k_1 * [H+]^a + \frac{k_2}{[H+]^b}, \quad (\mathrm{dm^3/mol})^{4.6}\mathrm{s}^{-1} \tag{5.2}$$

whereas k_0, k_1, and k_2 were described in equations (3.14) to (3.16) and values of k_{00}, k_{01}, k_{02}, E_0, E_1, and E_2 are listed in Table 5.1.

The reaction kinetics essentially consists of three regions: high, medium and low pHs. That the activation energy of the low pH region (E_2) is nearly half of that of the other regions while the rate constant of the low pH region is 6000 times greater than that of the medium region demonstrates that the reaction rate is strongly affected by the pH of the solution. This very important characteristic can be employed in controlling the rate of the reaction, or in other words, controlling the release of heat from the reaction.

5.2. Polymer Dissolution Kinetics

5.2.1. Effect of Coating Thickness

To examine the effect of the thickness of the Eudragit®S layer on the lag time, citric acid-loaded capsules (size #4 having length of 13 mm and diameter of 5 mm) were coated with 18 wt% solution of Eudragit®S in various coating thickness from 0 to 0.37 mm. The initial temperatures were kept at 4°C and 24°C while other parameters such as concentrations of the two reactants, size and number of capsules, volume of the reactive solution,

stirring speed, and amount of NaOH added or essentially the initial pH of the solution were maintained constant throughout the experiments.

As being expected, the lag time observed in the dissolution test in the reactive system was delayed with increased coating, and a very good linear relationship was found between the coating thickness and the lag time (Figure 5.3). This leads to three important findings:

- the onset time of catalyst release from the capsules could be controlled quantitatively over a quite wide range by altering the coating thickness of the Eudragit® S layer.
- the rate of dissolution of the polymer coat essentially does not depend on the thickness of the polymeric coat. In other words, depending on what mechanism dominates the dissolution, it will be merely a function of temperature, pH, and/or Reynold number (stirring speed, capsule size). Therefore, having kept all of those parameters constant, the rate of dissolution of the polymer can be determined by dividing the thickness of the coat by the lag time:

$$dissolution\ \ rate\ \ (\gamma) = -\frac{dl}{dt} = \frac{thickness\ \ of\ \ the\ \ coating}{lag\ \ time} = \gamma(T, pH, \mathrm{Re}) \tag{5.3}$$

  Hence, hereafter, the dissolution rate calculated from the above equation will be used to derive the rate expression of the polymer dissolution instead of the lag time.
- in the reaction-limited regime, the polymer dissolution rate is zero-order with respect to the polymer concentration (both ionized and unionized) at the surface of the coat. Consequently, the rate of polymer dissolution when reaction step is the rate-limiting step is:

$$\gamma = -\frac{dl}{dt} = kp[H^+]^{-q} \tag{5.4}$$

  where the rate constant, k, can be expressed in the Arrhenius form as in equation (3.18).

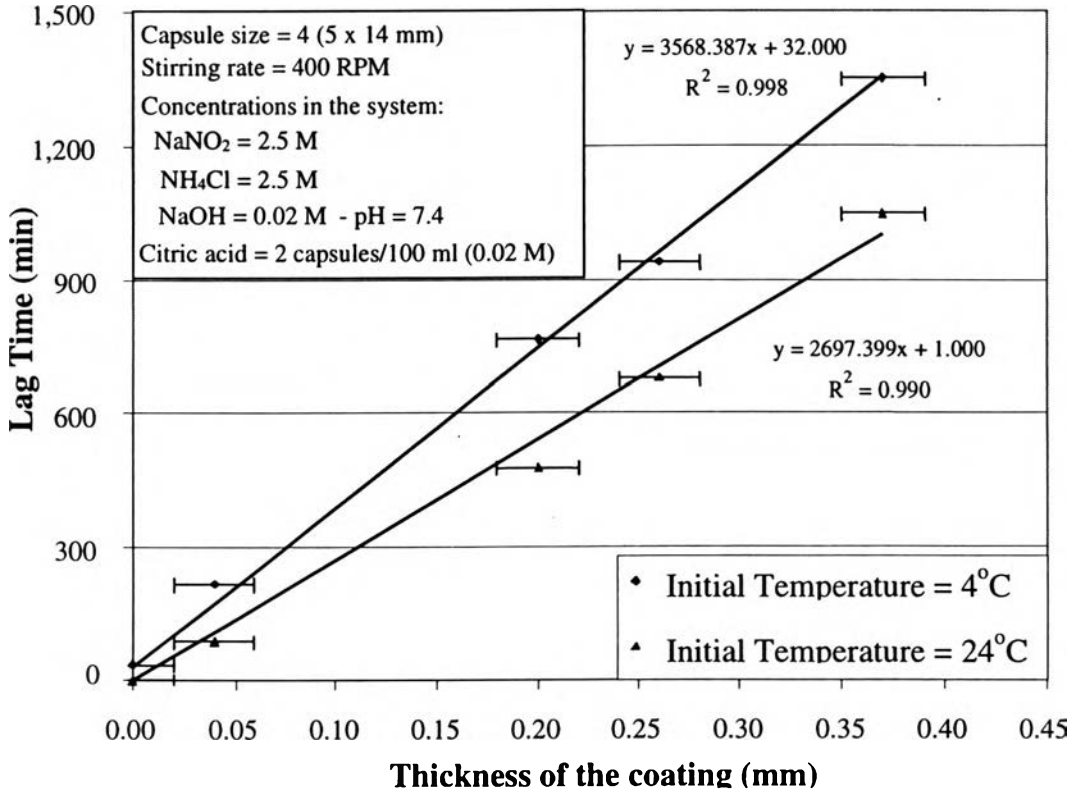

Figure 5.3 Effect of thickness of the coating to the lag time.

As a result of those findings, the dissolution rate (mm/h) at an initial adding amount of NaOH of 0.08 g/100 ml solution (corresponding to a solution's pH value of 7.4), a stirring speed of 400 rpm, a number of capsules of 2, a capsule size of 4, and initial temperatures of 4°C and 24°C were obtained by averaging dissolution rate at different thickness at those conditions as shown in Figure 5.4. From this study, the average values of the dissolution rate are 0.023 and 0.0163 mm/h at 24°C and 4°C, respectively. The results show that an increase in temperature increased the dissolution rate of the polymeric coat.

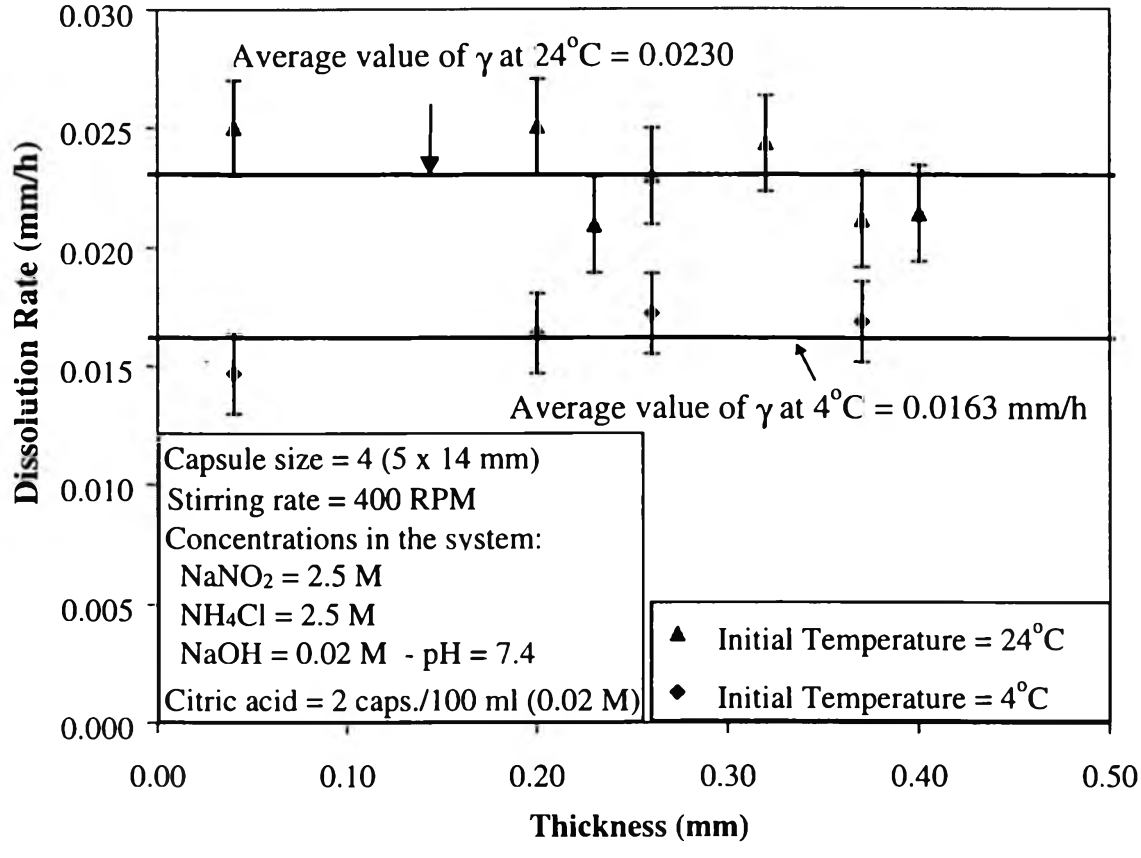

Figure 5.4 Average values of dissolution rate at 4°C and 24°C.

5.2.2. Effect of Mixing Degree

Next, the effect of mixing degree on the dissolution rate was studied in order to find out the mechanism of the polymer dissolution. The stirring speed of the magnetic bar was varied at 0, 100, 200, and 400 rpm while other parameters were kept constant. Figure 5.5 clearly shows that all the values of the dissolution rate at different degrees of mixing were similar in nature. Moreover, since the equivalent diameter of the polymer-coated capsule (7 mm) was in the same order of magnitude with the diameter of the reactor (30 mm), the operational range of stirring speed gave all flow regimes (no flow, laminar, and turbulent flow). Thus, it can be concluded that the polymer dissolution rate is independent of the flow regime of the surrounding solution. The dissolution of the polymeric coat is therefore limited by the ionization reaction at the polymer surface.

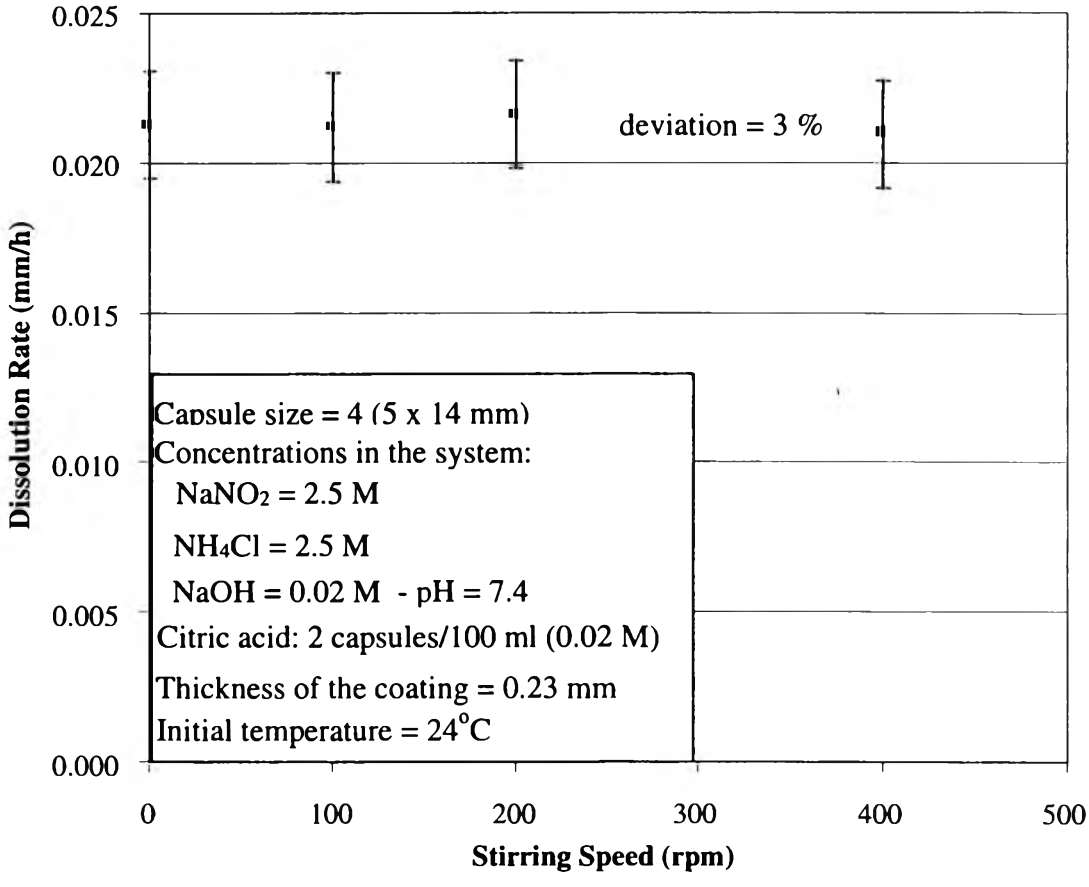

Figure 5.5 Effect of mixing on the polymer dissolution rate.

Eventually, this finding together with the finding about the effect of the thickness lead to the conclusion that the dissolution rate is merely a function of the concentration of proton and the temperature of the solution.

5.2.3. Effect of pH of the Solution

In order to determine the reaction order with respect to the concentration of proton in the solution, the pH of the solution was varied from 6.19 to 8.06 by adding a correspondent amount of sodium hydroxide (from 0 to 0.01 mole per liter of the reactive solution). From Figure 5.6 plotting log of dissolution rate versus log of concentration of proton, the reaction order with respect to $[H^+]$ was found to be –0.411. Hence, the rate of dissolution is inversely proportional to the concentration of H^+ in the solution which totally agrees with the theoretical mechanism proposed.

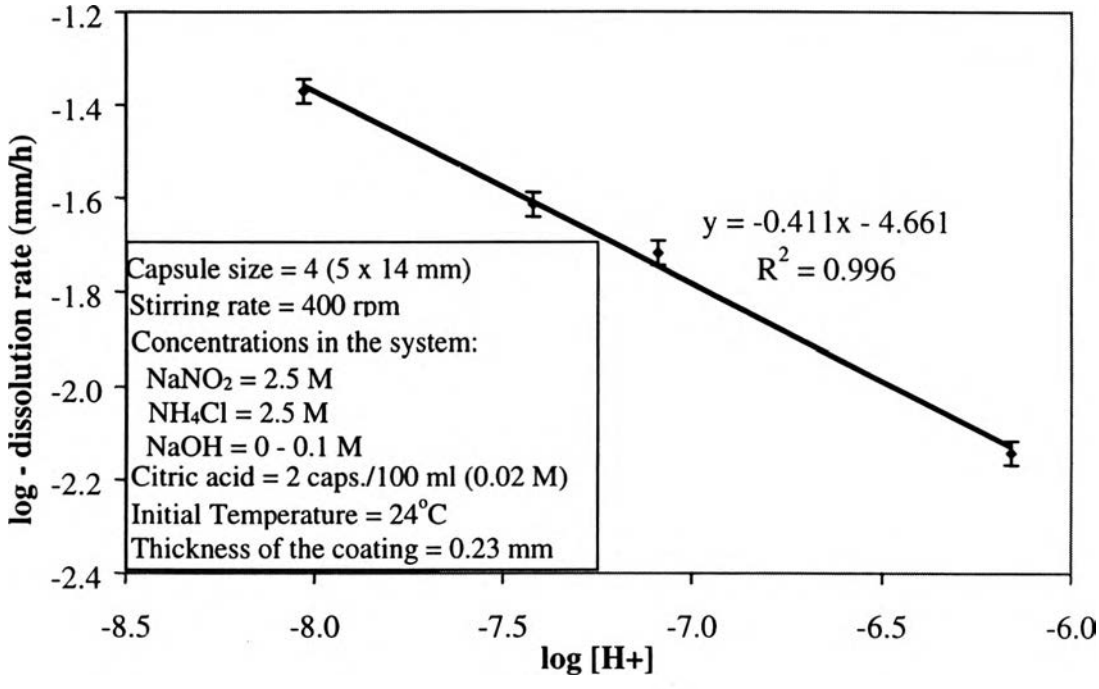

Figure 5.6 Effect of pH of the solution on the dissolution rate.

5.2.4. Effect of Temperature of the Solution

To obtain the dissolution constant and activation energy of the polymer dissolution rate, the initial temperature of the reactive solution was varied at 4°C, 24°C, and 34°C while the initial pH was kept constant. The rate constant, k, at those temperatures were then calculated from the dissolution rate using the reaction order with respect to $[H^+]$ found above. The natural log-log graph plotting dissolution rate versus temperature (Figure 5.7) reveals the rate constant expression of the polymer dissolution (ionization) following the Arrhenius expression (5.5) with the activation energy, Ep, of 2.3 kcal/mole, and rate constant kp_0 of 0.001 mm/h.

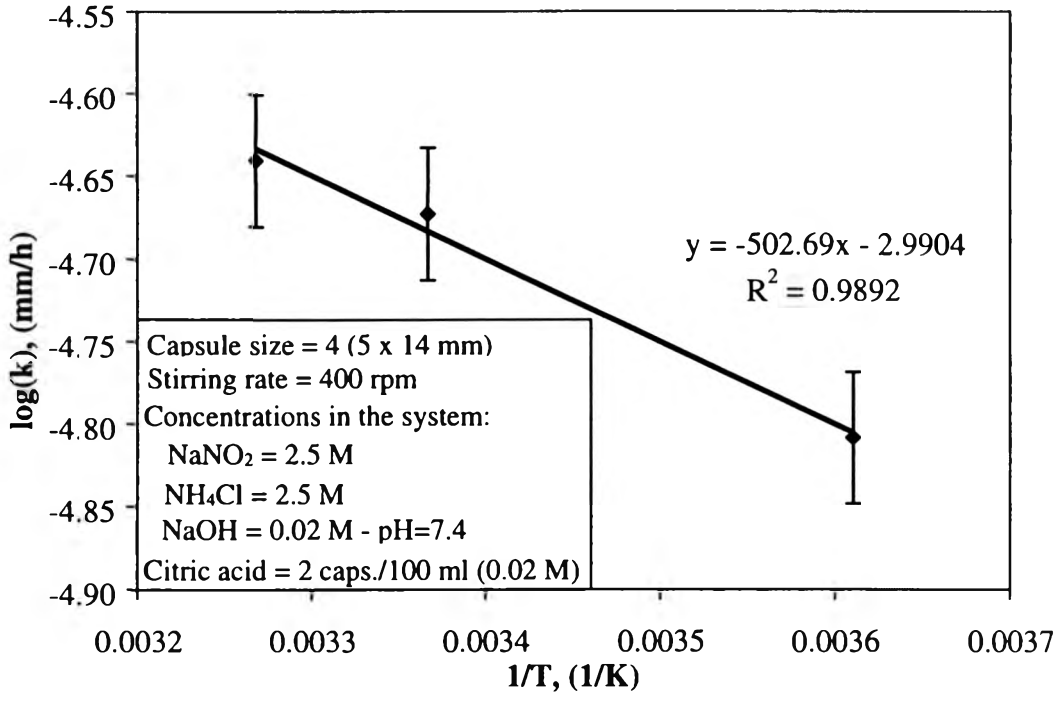

Figure 5.7 Effect of temperature on the polymer dissolution rate.

5.2.5. Effect of the Amount of Capsules per Unit Volume of Solution

The aim of studying the effect of the amount of capsules with basically the same thickness of polymeric coat per unit volume of solution was to double-check the polymer dissolution kinetics. According to the theoretical model proposed, the dissolution rate should not depend on the amount of capsules added to the reactive solution.

Moreover, one experiment was conducted in which 7 capsules with thickness of theirs coat being distributed from 0.23 mm to 0.30 mm. The purpose of this experiment was three-fold:

- to study the effect of the release of acid from one capsule to the dissolution of the others. This is an interesting effect which is necessary to be understood to do population balance simulation in a flowloop and/or a pipeline.

- to determine the effect of a distribution of coating thickness or a distribution of lag time and release time to the temperature-time profile in the batch reactor.
- to verify the kinetics of the polymer dissolution.

Figure 5.8 shows that the dissolution rate was independent of the amount of capsules with essentially the same thickness of polymeric coat added to the reactive solution. Moreover, in the case of 7 capsules having different thickness, the dissolution rate calculated by dividing the thickness of the least thick capsule by the lag time was similar to those in other cases. It can be concluded, then, that the lag time was determined by the least thick capsule; this result is consistent with the polymer dissolution kinetics and is very substantial for applying population balance theory in doing flowloop and/or pipeline simulation.

Since the ionization rate has a low activation energy (less than 3 kcal/mole), it is strongly dependent on the temperature of the solution. The rate, therefore, is expected to be very rapid at high temperature; this explains the result of the 7-capsule case. The capsules with thicker coating thickness were dissolved owing to the increase in temperature of the solution caused by the release of acid from the less coated capsules. However, observation of the capsules after reaction showed that not all the polymeric coat was dissolved. That is due to not only a decrease in pH of the solution but also the glassification and swelling of the polymer at high temperature.

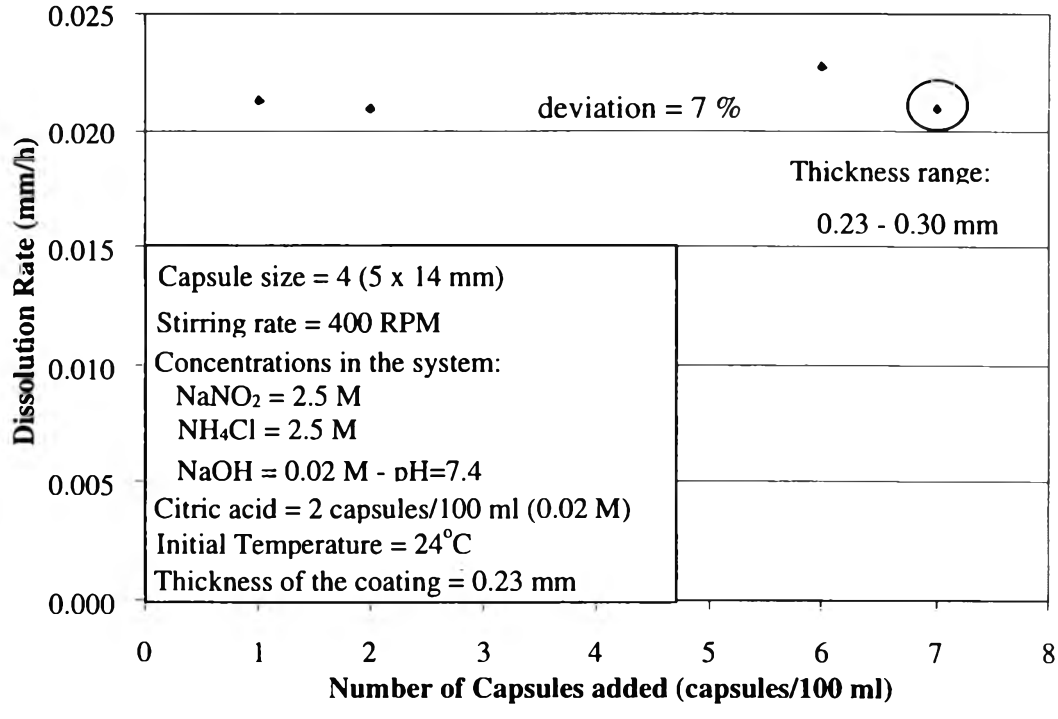

Figure 5.8 Effect of amount of capsules/100 ml on the dissolution rate.

5.3. Numerical Modeling

Having determined the kinetics of the reaction and the dissolution kinetics of the polymeric coat, temperature-time profiles of the reactive system in a batch reactor or temperature-distance profiles in a pipeline are now possible to model. Those profiles essentially consists of three regions:

1. The polymeric coat is dissolving at essentially the initial temperature and initial pH while the reaction occurs at a fairly slow rate thanks to the pretty high pH of the solution. This region is therefore the polymer dissolution region

2. The polymeric coat has been dissolved but not totally due to the uneven coating thickness; the acid is only released through a small area. Therefore, it will take a time for all the acid to be released and dissolve into the reactive solution. The pH of the solution gradually decreases then levels off leading to an increase in the rate of the exothermic reaction. However, the pH of the solution is not sufficiently low to trigger the reaction. Consequently,

this region is a transient region where the release of the catalyst from the capsule(s) determines the pH of the solution, and through which, the rate of the reaction.

3. The acid has been totally released, reducing the pH of the solution to such a low value that the reaction occurs at a sufficiently rapid rate to shoot up the temperature of the solution. This is the reaction-dominated region. The temperature increases until the boiling point of the solution is reached. After that, temperature of the solution starts declining due to the consumption of the reactants together with the loss of heat to the surrounding.

5.3.1. Assumptions

1. The dissolution of a particular capsule is not affected by the presence of other capsules, i.e, the capsules behave independently. However, a capsule, once dissolves, depending how much it influences the surrounding solution in terms of pH, does affect the dissolution of other capsules.

2. The release of the catalyst from a capsule is zero-order after one part of the polymeric coat has been dissolved and the catalyst is exposed to the solution. In other words, the catalyst is released linearly through a cavity on the capsule wall. The released catalyst is immediately dissolved and lowers the pH of the solution.

5.3.2. Methodology

The system of ordinary differential equations described in part 3.3 were solved by using fourth-order Runge-Kutta method.

5.3.3. Comparison between Simulation & Experimental Results for a Batch Reactor

The delay time, which is the time when temperature of the reactive solution starts to shoot up, was chosen as the main parameter to compare simulation results to experimental results. In addition, two typical temperature-time profiles were also selected to evaluate the similarities between the experimental and simulation results.

As shown in Figures 5.9 and 5.10, at the two initial temperatures of 4°C and 24°C, the two delay times at different thickness are quite similar. The deviations are probably due to the error in determination the rate constants and activation energies of the reaction kinetics as well as of the polymer dissolution kinetics.

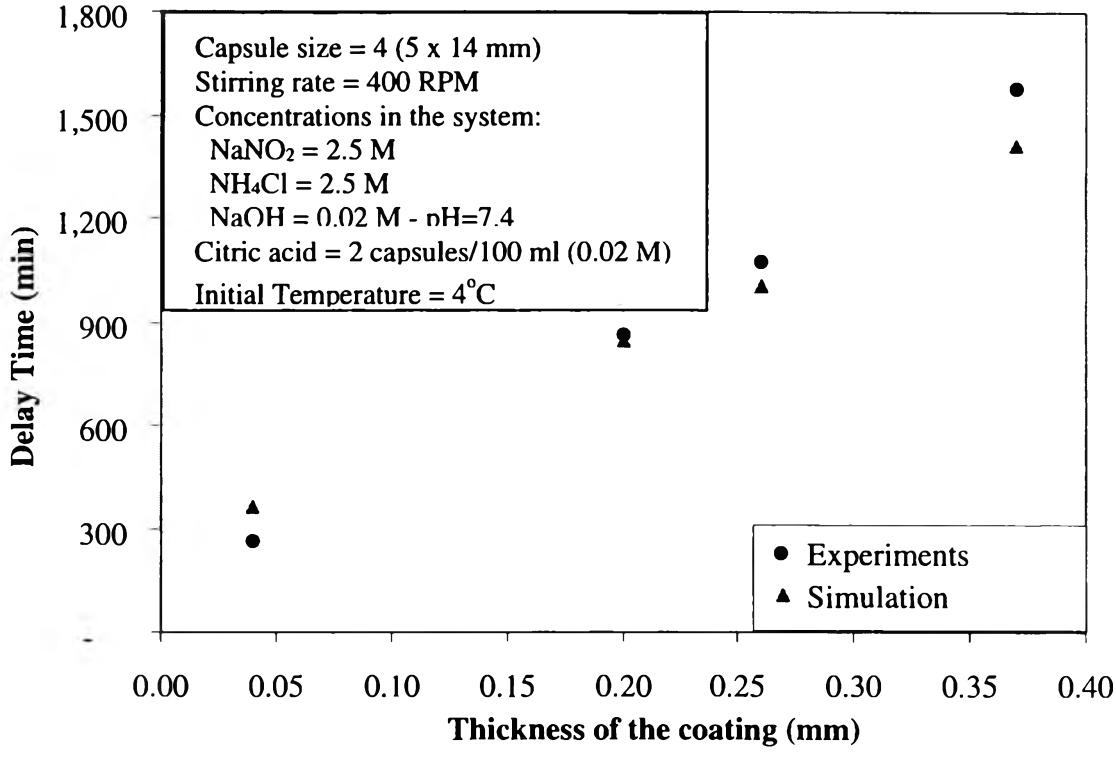

Figure 5.9: Calculated and observed delay time at temperature of 4°C.

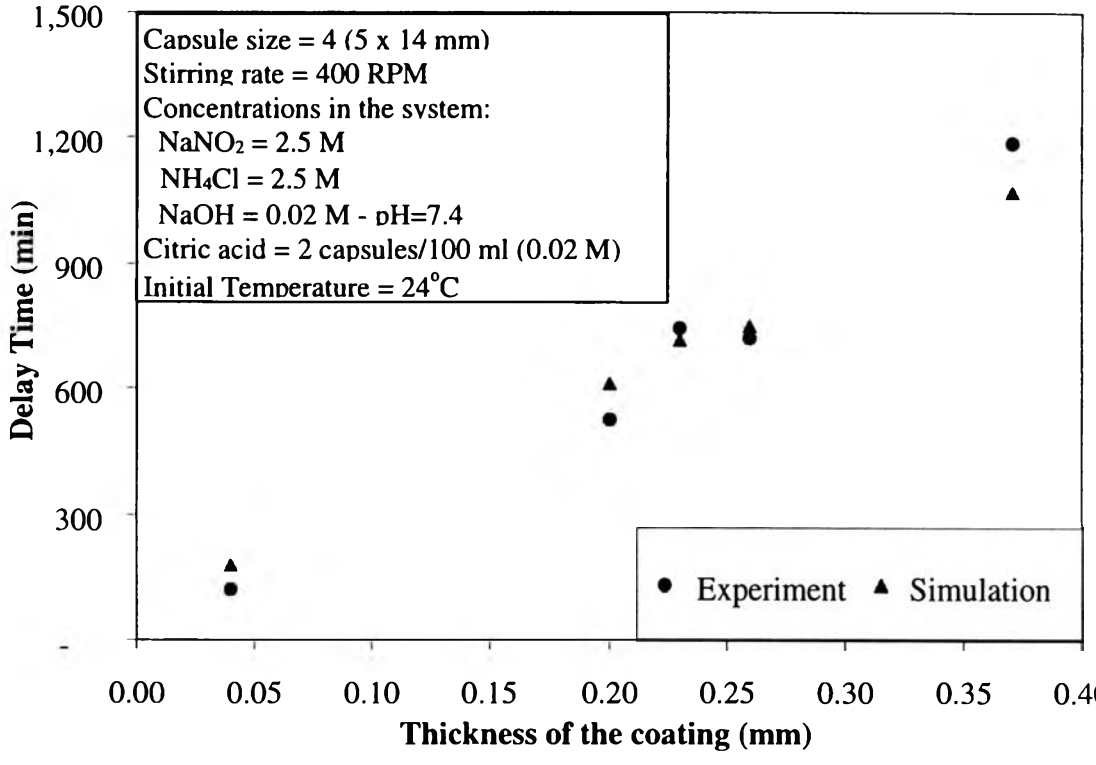

Figure 5.10: Calculated and observed delay time at temperature of 24°C.

The temperature-time profiles at initial temperature values of 4°C and 24°C from experiments and simulation at a coating thickness of 0.26 mm were compared in Figure 5.11. The simulated temperature-time profiles with adjustment counting for the heat loss to the surrounding are quite agreed in nature and in fact, have nearly identical parameters such as delay time and rate of increasing temperature with the experimental profiles. The agreement both in the delay times obtained and the temperature-time profiles clearly show that the kinetics of the exothermic reaction as well as of the polymer dissolution found are entirely reasonable and the reaction in a batch reactor was successfully modeled.

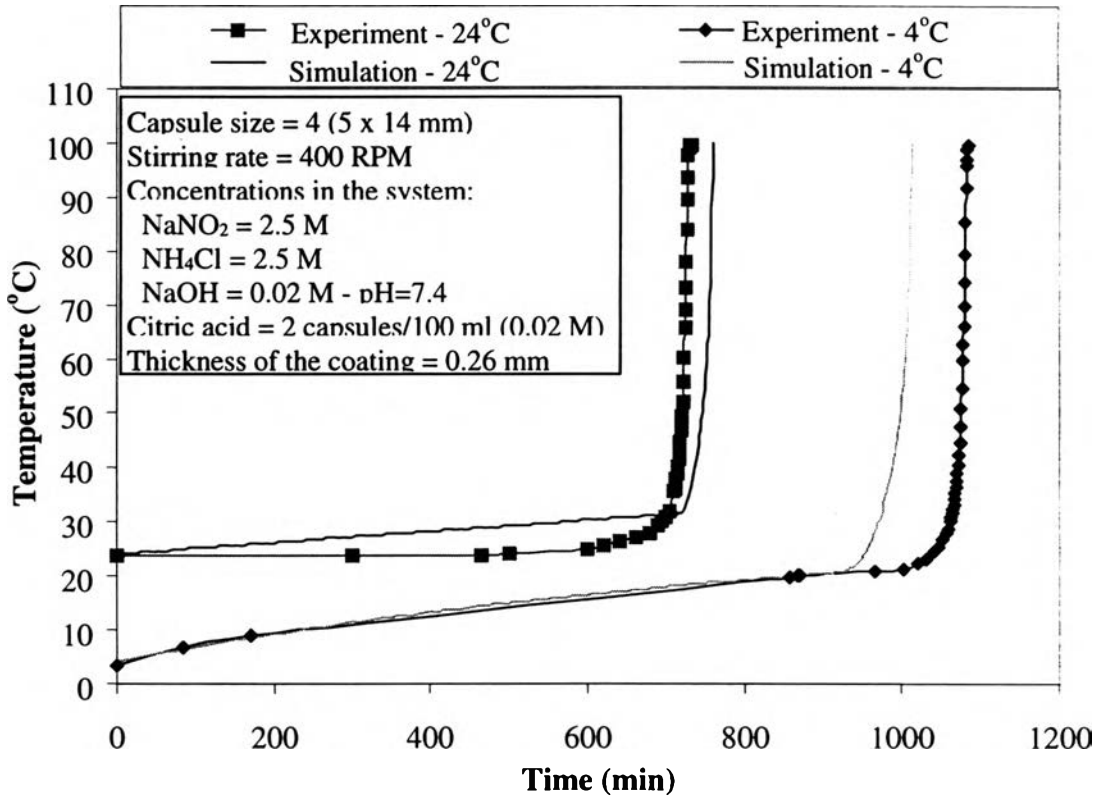

Figure 5.11: Calculated and observed temperature-time profiles.

5.3.4. Simulation for a Pipeline

Having verified the reaction kinetics and polymer dissolution kinetics in a batch reactor through comparing the temperature-time profiles and the delay time, one can now evaluate the feasibility of the encapsulation technique using together with fused chemical reaction method to provide heat to further regions in a pipeline. The calculated temperature-distance profile in a sub-sea pipeline at steady state for a polymeric coating thickness of 0.26 mm (figure 5.12) clearly demonstrates that the encapsulation technique is excellent in controlling the exothermic reaction. The release of heat from the reactive system could be delayed up to 60 kilometers in the pipeline at a polymeric coating thickness of 0.26 mm and normal operating conditions (velocity: 1 m/s). The reaction is then capable of providing sufficient amount of heat to raise and maintain the temperature of the solution at a level of more than the minimum effective limit (around 50°C) for a length range from 80 to 105

kilometer in the pipeline. Moreover, the temperature of the reactive system was kept lower than the maximum limit temperature in that range; therefore, the inner and outer coating of the pipeline would not be adversely affected.

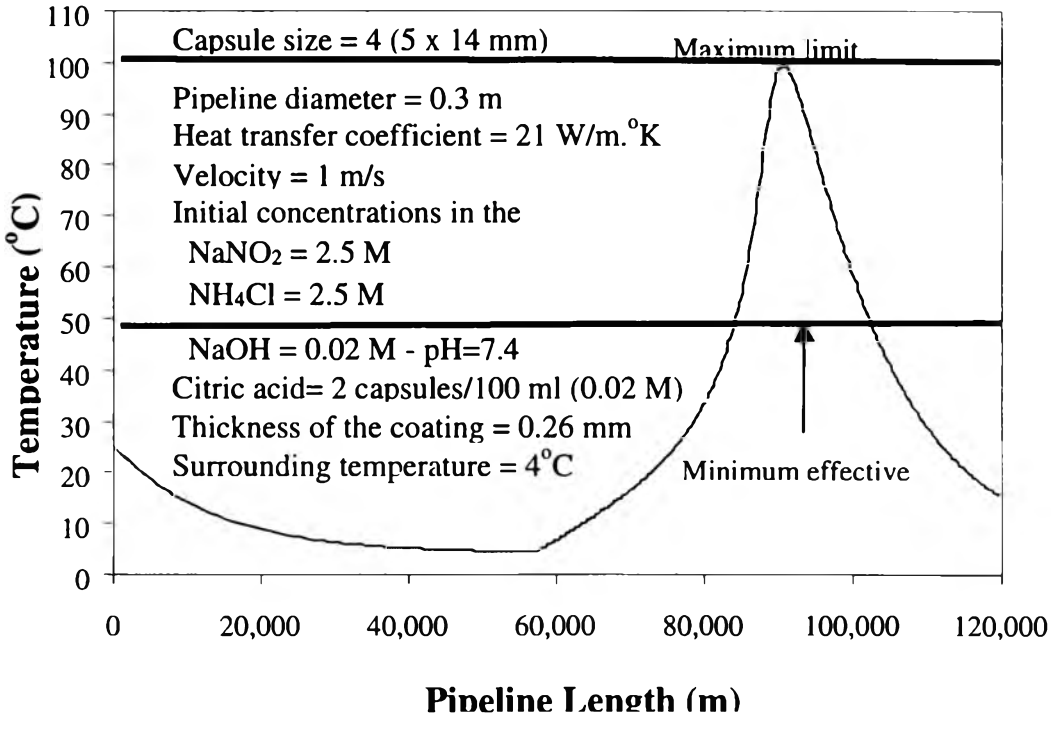

Figure 5.12: Calculated temperature-distance profile in a sub-sea pipeline at steady state.

Furthermore, when a flatter and longer temperature-distance profile is desired, a group of capsules with different polymeric coating thickness can be used to provide a pulse effect.